

Washington University School of Medicine

Digital Commons@Becker

---

2020-Current year OA Pubs

Open Access Publications

---

3-13-2023

## Allopregnanolone effects on inhibition in hippocampal parvalbumin interneurons

Xinguo Lu

Peter Lambert

Ann Benz

Charles F. Zorumski

Steven J. Mennerick

Follow this and additional works at: [https://digitalcommons.wustl.edu/oa\\_4](https://digitalcommons.wustl.edu/oa_4)



Part of the [Medicine and Health Sciences Commons](#)

Please let us know how this document benefits you.

---

## Neuronal Excitability

# Allopregnanolone Effects on Inhibition in Hippocampal Parvalbumin Interneurons

Xinguo Lu,<sup>1</sup> Peter Lambert,<sup>1</sup> Ann Benz,<sup>1</sup>  Charles F. Zorumski,<sup>1,2,3</sup> and  Steven J. Mennerick<sup>1,2,3</sup><https://doi.org/10.1523/ENEURO.0392-22.2023>

<sup>1</sup>Department of Psychiatry, Washington University in St. Louis, St. Louis, MO 63110, <sup>2</sup>Department of Neuroscience, Washington University in St. Louis, St. Louis, MO 63110, and <sup>3</sup>Taylor Family Institute for Innovative Psychiatric Research, Washington University in St. Louis, St. Louis, MO 63110

## Abstract

Allopregnanolone (AlloP) is a neurosteroid that potentiates ionotropic GABAergic (GABA<sub>A</sub>) inhibition and is approved for treating postpartum depression in women. Although the antidepressant mechanism of AlloP is largely unknown, it could involve selective action at GABA<sub>A</sub> receptors containing the  $\delta$  subunit. Despite previous evidence for selective effects of AlloP on  $\alpha 4/\delta$ -containing receptors of hippocampal dentate granule cells (DGCs), other recent results failed to demonstrate selectivity at these receptors (Lu et al., 2020). In contrast to DGCs, hippocampal fast-spiking parvalbumin (PV) interneurons express an unusual variant partnership of  $\delta$  subunits with  $\alpha 1$  subunits. Here, we hypothesized that native  $\alpha 1/\delta$  receptors in hippocampal fast-spiking interneurons may provide a preferred substrate for AlloP. Contrary to the hypothesis, electrophysiology from genetically tagged PV interneurons in hippocampal slices from male mice showed that 100 nM AlloP promoted phasic inhibition by increasing the sIPSC decay, but tonic inhibition was not detectably altered. Co-application of AlloP with 5  $\mu$ M GABA did augment tonic current, which was not primarily through  $\delta$ -containing receptors. Furthermore, AlloP decreased the membrane resistance and the number of action potentials of DGCs, but the impact on PV interneurons was weaker than on DGCs. Thus, our results indicate that hippocampal PV interneurons possess low sensitivity to AlloP and suggest they are unlikely contributors to mood-altering effects of neurosteroids through GABA effects.

**Key words:** antidepressant; inhibition; interneuron; neurosteroid

## Significance Statement

Allopregnanolone (AlloP) is an endogenous positive allosteric modulator of GABA<sub>A</sub> receptors and appears to have antidepressant effects triggered faster than traditional medications. The antidepressant mechanism of AlloP is largely unknown and we tested whether inhibition of parvalbumin (PV) interneurons in mouse hippocampus could participate. Our results indicate that PV interneurons possess low sensitivity to AlloP despite favorable receptor subunit composition.

## Introduction

Inhibition sculpts neurophysiological excitability and modulates oscillations in brain networks that give rise to sensation, perception, and cognition. In the mammalian CNS, most inhibition is mediated by GABA<sub>A</sub> receptors,

which are ligand-gated, chloride-permeable ion channels (Sigel and Steinmann, 2012). They are heteropentameric and composed of two  $\alpha$ , two  $\beta$ , and a fifth subunit, usually either  $\delta$  (extrasynaptic in certain cells) or  $\gamma 2$  (synaptic in most cells; Pirker et al., 2000; Wei et al., 2003). Subunits are assembled according to precise rules. For instance,  $\delta$  subunits preferentially co-assemble with  $\alpha 4$  or  $\alpha 6$  subunits in a select

Received September 18, 2022; accepted January 18, 2023; First published February 1, 2023.

C.F.Z. is a member of the Scientific Advisory Board for Sage Therapeutics. Sage Therapeutics had no role in the design or interpretation of the present experiments. All other authors declare no competing financial interests.

Author contributions: X.L., P.L., C.F.Z., and S.J.M. designed research; X.L., P.L., and A.B. performed research; X.L. and S.J.M. analyzed data; X.L., P.L., C.F.Z., and S.J.M. wrote the paper.

group of projection cell types, including dentate granule cells (DGCs) of the hippocampus ( $\alpha 4$  pairing). These  $\delta$ -containing receptors localize extrasynaptically, have high GABA sensitivity, and mediate tonic inhibition (Brown et al., 2002; Wei et al., 2003; Glykys et al., 2008) and some slow phasic inhibition (Herd et al., 2013; Sun et al., 2018; Shu et al., 2021). GABA is the neurotransmitter agonist of GABA<sub>A</sub> receptors and is released by GABAergic interneurons. Although perhaps underappreciated, GABAergic interneurons themselves express GABA<sub>A</sub> receptors and receive phasic and tonic inhibition from other interneurons (Pelkey et al., 2017). In contrast to more extensively studied projection cells, hippocampal interneurons, especially fast-spiking parvalbumin-positive (PV) interneurons, express an unusual variant partnership of  $\delta$  subunits with  $\alpha 1$  subunits (McDonald and Mascagni, 2004; Milenkovic et al., 2013; Hu et al., 2014).

Allopregnanolone (AlloP) is an endogenous neurosteroid that functions as a positive allosteric modulator to potentiate GABAergic inhibition (Harrison et al., 1987). AlloP, formulated as brexanolone/Zulresso, was recently approved for treating postpartum depression in women and has shown promise in major depressive disorder (Kanes et al., 2017; Gunduz-Bruce et al., 2019; Walton and Maguire, 2019). Although the overall benefit in humans and precise onset of any antidepressant action are still unclear, mechanisms through which AlloP act are of considerable interest, in part because onset is faster than conventional antidepressants.

A prevailing view is that neurosteroids, like  $3\alpha, 21$ -dihydroxy- $5\alpha$ -pregnan- $20$ -one (THDOC) and AlloP, selectively potentiate  $\delta$ -containing GABA<sub>A</sub>Rs to enhance tonic inhibition. The potentiating effect of neurosteroids is nearly abolished in  $\delta$  knock-out DGCs (Stell et al., 2003; Carver and Reddy, 2016). Further, the anesthetic effects of neurosteroids are strongly altered in  $\delta$  deficient mice (Spigelman et al., 2003). Finally, recent data suggest that  $\delta$ -containing PV interneurons in the basolateral amygdala may be important for the mood-altering effects of neurosteroids (Antonoudiou et al., 2022). Here, we explore hippocampal PV interneurons because of the role of the hippocampus in cognitive changes associated with many neuropsychiatric disorders and the previous association with antidepressant effects.

Previous studies, using novel pharmacoresistant GABA<sub>A</sub>R subtypes, showed that AlloP, while indeed augmenting inhibition, does not selectively potentiate classical  $\alpha 4/\delta$ -containing receptors to mediate tonic inhibition in hippocampal

DGCs compared with  $\gamma 2$ -containing receptors in the same cells (Lu et al., 2020). It is possible that noncanonical  $\delta$  pairings (e.g., with  $\alpha 1$  in PV interneurons) exhibit higher neurosteroid sensitivity than observed in DGCs. If that is the case, it could represent an important substrate of drug actions at the low concentrations thought to be therapeutically relevant.

We hypothesized that AlloP disinhibits principal cells by enhancing GABA<sub>A</sub>R function on PV interneurons, thereby inhibiting them and promoting excitability of principal neurons. We genetically tagged mouse PV interneurons and examined how these cells respond to AlloP during phasic and tonic inhibition. We find little evidence for AlloP potentiation of baseline tonic current and only mild potentiation of IPSCs and tonic current recorded from PV interneurons in the presence of GABA. The impact of AlloP on excitability of DGCs was stronger than on excitability in PV interneurons. By contrast, field EPSPs (fEPSPs) in CA1 were modestly potentiated by AlloP. Overall, the results preclude a large role for hippocampal interneuron GABA receptors, especially tonic inhibition in PV interneurons, in therapeutic AlloP effects.

## Materials and Methods

### Animals

Male mice of PVCre or Ai14::PVCre from postnatal day (P)30 to P60 were used. We failed to find a clear change in exogenous AlloP effect with age, as demonstrated in the data available on Figshare. We also examined two female mice, whose data appeared similar to that of males and are included in the data available on Figshare. Sibling animals were group housed in zeitgeber time (ZT) 12:12 conditions, with ZT0 = 6 A.M. PV interneurons were labeled using two approaches: viral injection of pAAV5-hSyn-DIO-EGFP (Addgene, 50 457) into hippocampus of PVCre animals or Ai14::PVCre reporter mice (Ai14, Jackson Lab 007914; PVCre, Jackson Lab 017320). We assessed reporter accuracy with immunostaining against PV in Ai14 mice (Fig. 1). PV antibody (mouse anti-PV, P3088, Millipore Sigma) co-labeled 73% of tdTomato-positive cells (190 cells counted), consistent with precedent hippocampal assessments (Ledri et al., 2014). To isolate GABA current mediated by  $\delta$ -containing GABA<sub>A</sub> receptors, we used picrotoxin (PTX)-resistant knock-in line ( $\delta^*$  KI; Sun et al., 2018). To eliminate current mediated by  $\delta$ -containing GABA<sub>A</sub> receptors in PV interneurons, *Gabrd* floxed mice (Lee and Maguire, 2013) were bred to PVCre mice to knock out  $\delta$ -containing GABA<sub>A</sub> receptors [conditionally knocked out (cKO)]. In some experiments, general interneuron populations were identified by pAAV1-mDlx-NLS-mRuby2 (Addgene, 99130; Dimidschstein et al., 2016).

### Slice preparation

Mice were anesthetized with isoflurane and decapitated according to protocols approved by the Washington University IACUC. Coronal brain slices (300- $\mu$ m thickness) were cut using a Leica VT1200 vibratome. During slicing, slices were maintained in ice-cold, modified

This work was supported by National Institutes of Health Grants R01MH123748, P50MH122379, and F30MH126548.

Acknowledgments: We thank Dr. Jamie Maguire, Tufts University, for the floxed *Gabrd* mice; Dr. Jin-Moo Lee, Washington University, for the Parvalbumin-Cre mice; and Dr. Vijay Samineneni, Washington University, for the Ai14 mice.

Correspondence should be addressed to Xinguo Lu at xinguolu@wustl.edu or Steven J. Mennerick at menneris@wustl.edu.

<https://doi.org/10.1523/ENEURO.0392-22.2023>

Copyright © 2023 Lu et al.

This is an open-access article distributed under the terms of the Creative Commons Attribution 4.0 International license, which permits unrestricted use, distribution and reproduction in any medium provided that the original work is properly attributed.

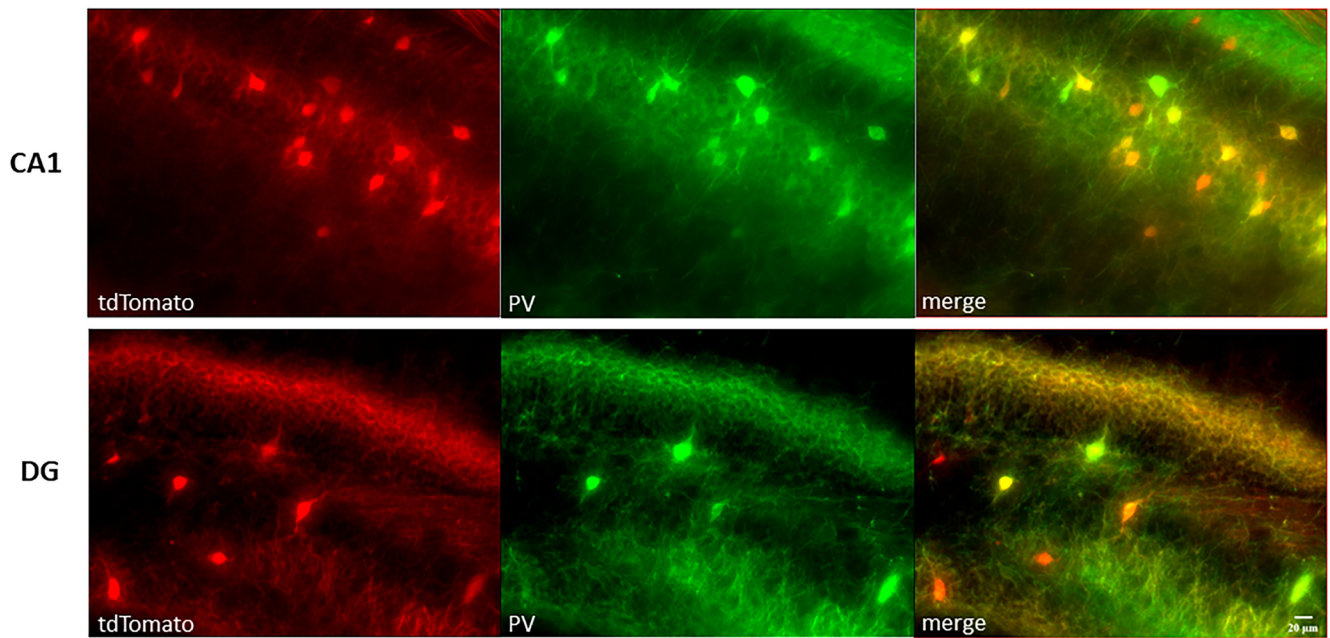


**Figure 1.** tdTomato fluorescence is a reliable indicator of PV interneurons in hippocampal CA1 and dentate gyrus from Ai14::PVCre mouse tissue. Top images, CA1. Bottom images, DG (dentate gyrus). Scale bar: 20  $\mu\text{m}$ .

NMDG-HEPES recovery artificial CSF (aCSF; in mM: 92 NMDG, 2.5 KCl, 1.25  $\text{NaH}_2\text{PO}_4$ , 30  $\text{NaHCO}_3$ , 20 HEPES, 25 glucose, 2 thiourea, 5 Na-ascorbate, 3 Na-pyruvate, 0.5  $\text{CaCl}_2$ , and 10  $\text{MgSO}_4$ ; 300 mOsm; pH 7.3–7.4). After slicing, slices recovered in modified NMDG-HEPES recovery aCSF at 32°C, and a  $\text{Na}^+$ -rich spike-in solution (4 ml, 2 M) was added to gradually increase  $\text{Na}^+$  concentration to improve the success of gigaseal formation (Ting et al., 2018). After recovery, slices were stored in modified HEPES holding aCSF (in mM: 92 NaCl, 2.5 KCl, 1.25  $\text{NaH}_2\text{PO}_4$ , 30  $\text{NaHCO}_3$ , 20 HEPES, 25 glucose, 2 thiourea, 5 Na-ascorbate, 3 Na-pyruvate, 2  $\text{CaCl}_2$ , and 2  $\text{MgSO}_4$ ; 300 mOsm; pH 7.3–7.4) for at least 1 h at 25°C before experimental recording. Drugs were obtained from ThermoFisher Scientific/MilliporeSigma except where noted.

### Whole-cell recording

During recording, slices were transferred to a recording chamber with continuous perfusion (2 ml/min, 32°C) of oxygenated, regular aCSF (in mM: 125 NaCl, 25 glucose, 25  $\text{NaHCO}_3$ , 2.5 KCl, 1.25  $\text{NaH}_2\text{PO}_4$ , equilibrated with 95% oxygen-5%  $\text{CO}_2$  plus 2  $\text{CaCl}_2$ , and 1  $\text{MgCl}_2$ ; 310 mOsm). IR-DIC microscopy (Nikon FN1 microscope and Photometrics Prime camera) was used to visualize and identify target cells during somatic, whole-cell recording. Borosilicate glass pipettes (World Precision Instruments, Inc) with open tip resistance of 3–6  $\text{M}\Omega$  were used for whole-cell recording. Cells were recorded with a MultiClamp 700B amplifier (Molecular Devices), Digidata 1550 16-bit A/D converter, and pClamp 10.4 software (Molecular Devices). A 5-min stabilization period followed initial break-in before recordings commenced.

To record action potentials, neurons were recorded in current-clamp mode using pipettes filled with K-gluconate

internal solution (in mM: 140 K-gluconate, 4  $\text{MgCl}_2$ , 10 HEPES, 0.4 EGTA, 4 MgATP, 0.3 NaGTP, and 10 phosphocreatine; pH was adjusted with KOH to pH 7.25; 290 mOsm). Step currents from  $-50$  pA with increments of 20 pA were injected to measure membrane properties and to elicit action potentials. Maximum firing frequency and action potential half width were calculated using Clampfit. For percentage accommodation, the 13th to 14th action potential interval was divided by the 3rd to 4th action potential interval. For cells that had fewer than 14 action potentials, the last and first intervals were used instead. To calculate membrane resistance, the steady-state voltage change in response to  $-50$ -pA step current was measured, and resistance was calculated by Ohm's Law.

To record phasic and tonic GABAergic current, 10  $\mu\text{M}$  NBQX (Tocris Bioscience) and 50  $\mu\text{M}$  D-APV (Tocris Bioscience) were added in the regular aCSF to inhibit ionotropic glutamate receptors. Pipettes were filled with cesium chloride internal solution (in mM: 130 CsCl, 10 HEPES, 5 EGTA, 2 MgATP, 0.5 NaGTP, and 4 QX-314; pH adjusted to 7.3 with CsOH; 290 mOsm). Cells were patched at  $-70$  mV in voltage-clamp gap-free mode at 5 kHz, filtered at 2 kHz using eight-pole Bessel filter.

### Field EPSP recording

To record population spikes in CA1, a bipolar stainless-steel stimulus electrode was placed in the Shaffer collaterals, and a glass recording electrode (blunt patch electrode) containing regular aCSF was placed in stratum pyramidale. For field EPSP recordings, electrodes were placed in stratum radiatum. A pulse (80  $\mu\text{s}$  wide) was applied to elicit EPSPs. A stimulus intensity (50–200  $\mu\text{A}$ ) to

elicit 50–60% of the maximum EPSP or population spike was used for data collection. In dentate gyrus, EPSPs were measured from lateral perforant pathway stimulation by placing the stimulus electrode and recording electrode in the outer molecular layer of the dentate gyrus, which were confirmed by paired-pulse facilitation (paired-pulse ratio  $1.38 \pm 0.29$  at a 50-ms stimulus interval; Froc et al., 2003). To ensure that AlloP fully reached the target cells, currents, action potentials, and fEPSPs were acquired 4 min after AlloP application. Any slice with baseline drift (EPSP of last minute vs first minute) over 20% was eliminated from analysis.

### Experimental design and statistical analyses

For sIPSCs measurement, templates were first created by average >50 events, and sIPSCs were detected using the template-matching algorithm in Clampfit (pClamp suite). At least 50 events contributed to average sIPSC waveforms in each experimental condition. sIPSC decays were fit to the sum of two exponential functions, extrapolated to the peak IPSC. Decay time course is reported as a weighted time constant ( $\tau_w$ ; Sun et al., 2018). For tonic GABA<sub>A</sub> currents measurements, mean holding currents with 200 ms in length during baseline and each drug condition were calculated when they reached steady state. Tonic GABA<sub>A</sub> currents were obtained by subtracting aCSF baseline holding currents. SD of the holding currents was calculated using Clampfit. Power analyses were used on pilot datasets to generate target N values. A paired *t* test or ANOVA as appropriate was performed using GraphPad Prism 8 or 9 to test effects within and among cells. For fEPSP recordings in CA1 stratum radiatum and dentate gyrus, the fEPSP rising slope was calculated in Clampfit. For field recordings in CA1 stratum pyramidale, the peak of the population spike was measured, or alternatively the form of EPSP was measured by the coastline burst index (CBI) as described (Widman and McMahon, 2018). Paired *t* tests were applied to compare the fEPSP rising slope or population spike during the last minute of drug application and during the last minute of baseline recording using GraphPad Prism 8 or 9. Specific analyses and exact *p* values are described in the figure legends. Statistical comparisons are presented at the level of ns not significant, \**p* ≤ 0.05, \*\**p* ≤ 0.01, \*\*\**p* ≤ 0.001, and \*\*\*\**p* ≤ 0.0001 in figures.

## Results

### Identification of fast-spiking PV interneurons

Because PV interneurons, aside from DGCs, represent the most  $\delta$  subunit-rich cell type in the hippocampus (Struble et al., 1978; Freundl and Buzsáki, 1996), we enriched for them in recording using either viral injection of pAAV5-hSyn-DIO-EGFP into hippocampi of Pv-Cre mice or the Pv-Cre line crossed to Ai14 reporter mice. A typical example of co-labeling for td-Tomato (Ai14) and PV immunostaining is shown in Figure 1 and summarized in Materials and Methods. To further confirm the phenotype of labeled cells, we characterized the firing patterns of PV interneurons. A depolarizing current was injected to elicit

action potentials in labeled PV interneurons, non-PV interneurons identified either by pAAV1-mDlx-NLS-mRuby2 virus (Dimidschstein et al., 2016) or by anatomic localization (somas in the molecular layer and hilar regions of the dentate and the stratum radiatum of CA1), and DGCs, identified anatomically by somas residing in the dentate granule cell layer (Fig. 2A–C). As expected, PV interneurons showed fast-spiking behavior with a maximum frequency near 200 Hz (Fig. 2D). Also, isolated action potentials of PV interneurons were briefer than those of non-PV interneurons and DGCs, with a half-width <0.5 ms (Fig. 2E). Finally, PV interneurons showed little accommodation compared with the other two cell groups (Fig. 2F). Taken together, the results show that reporter fluorescence enriches for PV interneurons.

### AlloP promotes phasic but not tonic inhibition on hippocampal PV interneurons

To test our hypothesis of AlloP effects on hippocampal interneuron  $\delta$ -containing GABA<sub>A</sub> receptors, we characterized the impact of AlloP on inhibition in PV interneurons. Whole-cell patch clamp was performed on PV interneurons, and both phasic and tonic currents were measured (Fig. 3A,I). 100 nM AlloP prolonged the decay of sIPSC from 3.7 to 4.8 ms (Fig. 3B). Neither the peak amplitude nor the frequency of sIPSCs was altered by AlloP (Fig. 3C, D). Surprisingly, 100 nM AlloP did not induce or amplify tonic current in PV interneurons (Fig. 3J). Additionally, the SD of tonic current, a sensitive proxy for tonic current (Lu et al., 2020) was not increased by AlloP (Fig. 3K). SD of the currents was reduced by 100  $\mu$ M PTX, indicating inhibition of basal GABA<sub>A</sub> receptor function that was not sensitive to augmentation by AlloP (Fig. 3K). To summarize, AlloP potentiated the phasic inhibition on PV interneurons by increasing the decay of sIPSC, but tonic inhibition was not potentiated by AlloP.

To place these results in context, we previously found that under the same experimental conditions, AlloP potentiates tonic GABA current in DGCs (Lu et al., 2020). Combined with results mentioned above, this suggests that DGCs and PV interneurons are differentially affected by tonic inhibition and AlloP under basal conditions. Here, we extended the comparison to include CA1 pyramidal neurons. AlloP prolonged IPSC decays as for PV interneurons and DGCs (Fig. 3E,F; Lu et al., 2020). If AlloP impacts the excitability of PV interneurons through inhibition from  $\delta$ -containing GABA<sub>A</sub> receptors, AlloP might decrease sIPSC frequency in CA1 pyramidal cells. However, we failed to detect an effect of AlloP on CA1 sIPSC frequency (Fig. 3G). Furthermore, selective deletion of the  $\delta$  subunit from PV interneurons ( $\delta$  cKO) failed to alter the baseline frequency of sIPSCs or the effect of AlloP on sIPSC waveform in CA1 pyramidal neurons (Fig. 3F–H), suggesting a negligible role for PV  $\delta$ -containing GABA<sub>A</sub> receptors on phasic inhibition in CA1 pyramidal neurons.

Previous work has shown that tonic current in CA1 pyramidal neurons is relatively insensitive to direct neurosteroid application; THDOC at low concentration did not potentiate either phasic or tonic inhibition in CA1 pyramidal neurons (Stell et al., 2003), although effects of neurosteroids in CA1 pyramidal neurons may be sex and age

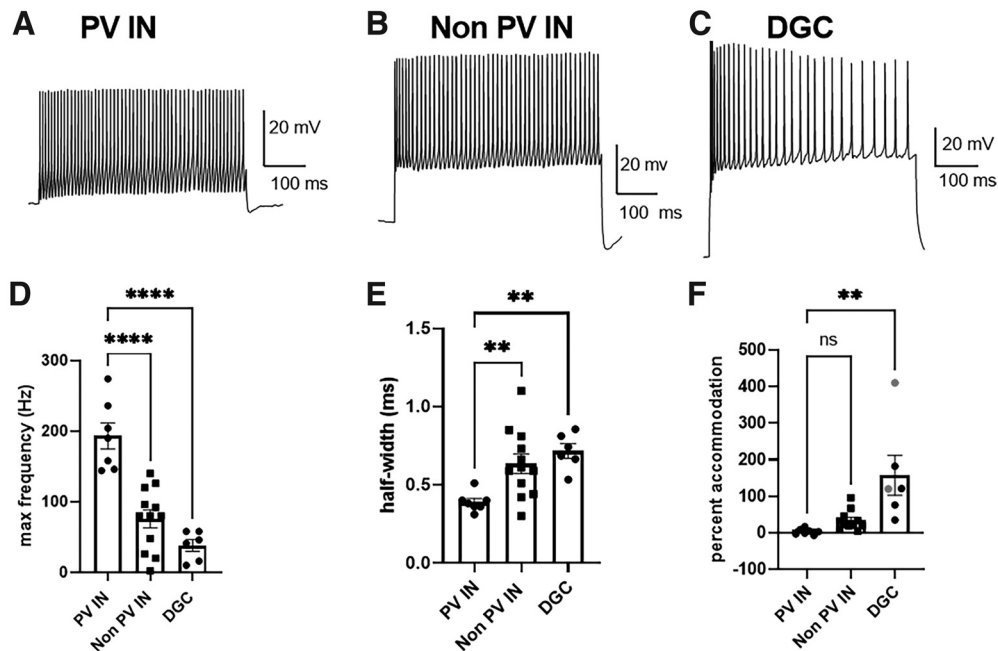


**Figure 2.** Action potential characteristics and repetitive firing patterns in fluorescent neurons readily distinguish seven PV interneurons (IN) from 12 non-PV interneurons (Non PV IN) and six DGCs. **A–C**, Representative voltage traces induced by depolarizing current injection. **D**, Maximum action potential frequency obtained by incremental increases in current amplitude from  $-50$  to  $400$  pA. One-way ANOVA showed a cell type effect ( $F_{(2,22)} = 26.49$ ,  $p < 0.0001$ ). PV interneurons had a higher maximum firing frequency than non-PV interneurons and DGC (Holm–Sidak,  $p < 0.0001$  for both). **E**, Half-width of action potentials elicited by just supra-threshold current injection. One-way ANOVA showed a main effect of cell type ( $F_{(2,22)} = 7.25$ ,  $p = 0.004$ ). PV interneurons had a smaller half-width than non-PV interneurons and DGC (Holm–Sidak,  $p = 0.005$  and  $p = 0.004$ , respectively). **F**, Percent accommodation of action potentials at maximum firing frequency. One-way ANOVA showed a genotype effect ( $F_{(2,21)} = 9.431$ ,  $p = 0.001$ ). PV interneurons had larger accommodation than DGC (Holm–Sidak,  $p = 0.001$ ), but not non-PV interneurons (Holm–Sidak,  $p = 0.362$ ). The red symbols indicate two cells in which the requisite number of action potentials was not exceeded (see Materials and Methods), so the time between the final two action potentials was taken as a minimum accommodation measure.

dependent (Smith et al., 2009). In our experiments, AlloP did not induce detectable tonic current in CA1 pyramidal neurons (Fig. 3L–N). However, as in PV interneurons, PTX reduced tonic current SD with PTX application (Fig. 3N), suggesting a small GABA<sub>A</sub>R mediated conductance that proved insensitive to AlloP.

### AlloP promotes tonic inhibition of PV interneurons with exogenous GABA

The results of Figure 3 indirectly suggest that  $\delta$ -containing receptors in PV cells may not mediate effects of low neurosteroid concentrations in hippocampus. However, Figure 3 shows that there is little basal tonic current in hippocampal PV cells on which AlloP can act. Because  $\alpha 1/\delta$  receptors, thought to characterize PV cells, show lower GABA sensitivity than  $\alpha 4/\delta$  receptors of DGCs (Jia et al., 2005),  $\delta$ -containing receptors may not contribute much to basal tonic current in PV cells. To determine whether addition of exogenous GABA might increase AlloP's effects, we applied  $5 \mu\text{M}$  GABA to enhance tonic current before application of AlloP in wild-type (WT) PV interneurons (Fig. 4A). GABA increased tonic current by  $\sim 10$  pA, and GABA presence unmasked AlloP potentiation of the tonic current (Fig. 4B,C, left).

To determine whether this GABA/AlloP potentiated tonic current is mediated by  $\alpha 1/\delta$  receptors, we used two

independent mouse lines. First, we separated tonic currents mediated by  $\delta$  and non- $\delta$  receptors in PV interneurons using PTX-resistant  $\delta^*$  KI mice (Sun et al., 2018; Lu et al., 2020) bred to Ai14 reporter mice. In fluorescent PV cells, PTX reduced a large portion of tonic current, suggesting a contribution of non- $\delta$  receptors to the GABA/AlloP tonic current (Fig. 4B,C, middle). Furthermore, we applied GABA/AlloP in PV interneurons with  $\delta$ -containing receptors conditionally knocked out (cKO). On average there was  $-18$ -pA tonic current induced in the absence of  $\delta$  receptors (Fig. 4B,C, right), not different from WT PV cells. Overall, our results showed that with exogenous GABA, AlloP promotes the tonic inhibition of hippocampal PV interneurons, but the effect is not dominated by  $\delta$ -containing receptors.

### AlloP decreases the firing frequency of DGCs with little impact on PVs

The results through Figure 4 suggest that AlloP may have little impact on excitability of hippocampal PV interneurons through tonic current. To test directly whether AlloP alters excitability, we administered  $100$  nM AlloP and measured the change of action potential firing frequency using step current injections in whole-cell, current-clamp recordings of PV interneurons. We used

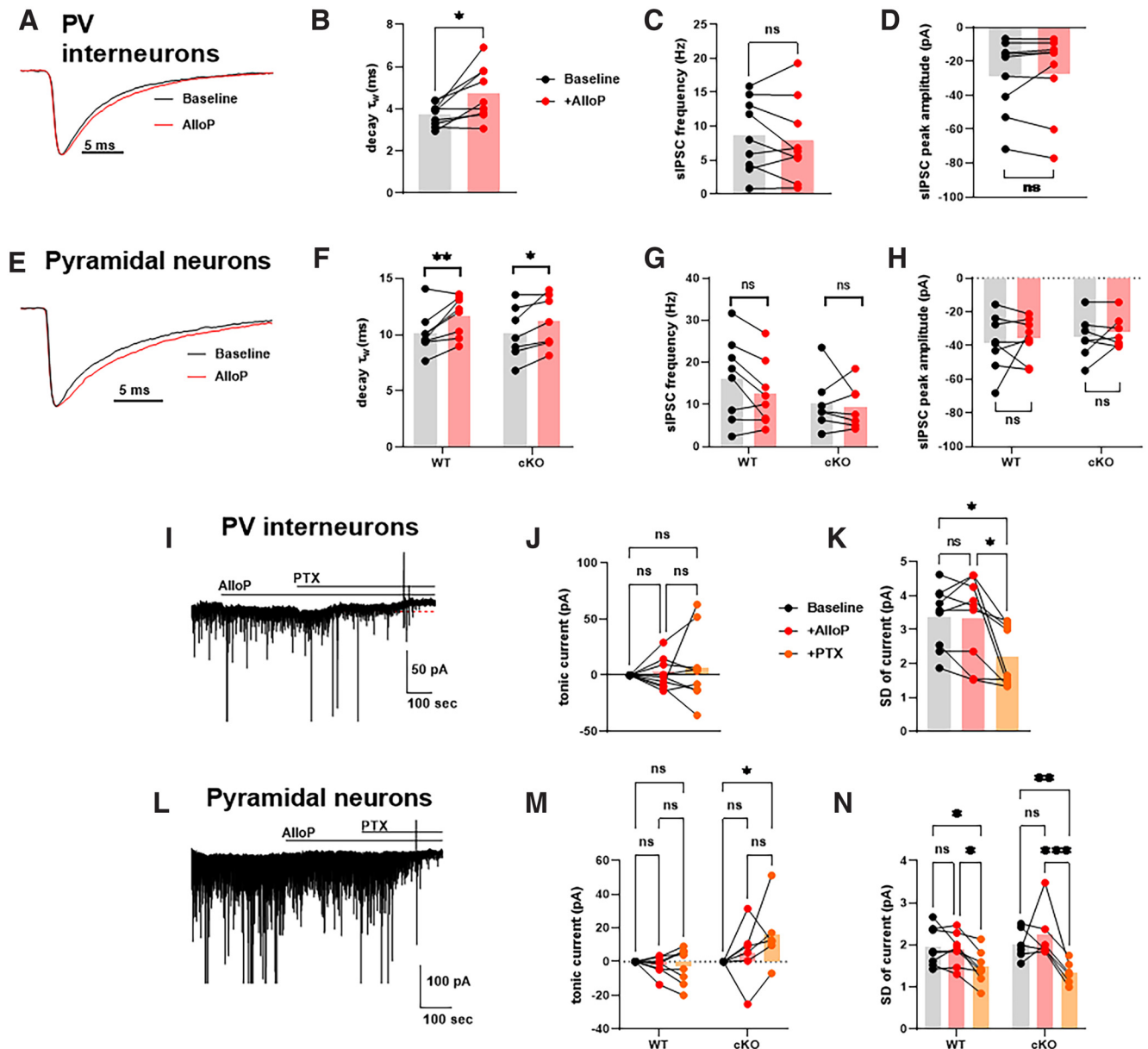


**Figure 3.** AlloP promotes phasic but not tonic inhibition in hippocampal PV interneurons and CA1 pyramidal neurons. **A**, Representative average sIPSC waveform from a PV interneuron at baseline (black trace) and after 100 nM AlloP application (red trace). **B–D**, sIPSC characteristics of PV interneuron ( $N=9$ ): **(B)** weighted decay  $\tau_w$  of sIPSC (paired  $t$  test,  $p=0.015$ ; \*), **(C)** frequency (paired  $t$  test,  $p=0.392$ ; ns), and peak amplitude (paired  $t$  test,  $p=0.663$ ; ns). **E**, Representative average sIPSC waveform from a CA1 pyramidal cell at baseline (black trace) and after 100 nM AlloP application (red trace). **F–H**, CA1 pyramidal neuron sIPSC characteristics of WT ( $N=8$ ) and  $\delta$  cKO ( $N=7$ ). **F**, Two-way ANOVA showed a drug effect on the weighted decay  $\tau_w$  of sIPSC ( $F_{(1,13)}=20.05$ ,  $p=0.0006$ ). AlloP increased  $\tau_w$  of sIPSCs in WT and cKO (Holm–Sidak’s test,  $p=0.004$  and  $0.024$ , respectively). **G**, Two-way ANOVA showed no drug effect on the frequency of sIPSC ( $F_{(1,13)}=3.26$ ,  $p=0.094$ ). AlloP had no effect on frequency of sIPSC in WT and cKO (Holm–Sidak’s test,  $p=0.099$  and  $0.652$ , respectively). **H**, Two-way ANOVA showed no drug effect on the amplitude of sIPSC ( $F_{(1,13)}=0.725$ ,  $p=0.41$ ). AlloP had no effect on amplitude of sIPSCs in WT and cKO (Holm–Sidak’s test,  $p=0.76$  and  $0.76$ , respectively). **I**, Effects of 100 nM AlloP on the holding current in a PV interneuron at  $-70$  mV. **J**, Summary of PV interneuron tonic current ( $N=9$ ). There was no discernible drug effect on the tonic current (one-way ANOVA,  $F_{(1,307,10.45)}=0.336$ ,  $p=0.632$ ). There was no difference in tonic current between baseline and AlloP, AlloP and PTX, baseline and PTX (Holm–Sidak’s test,  $p=0.906$ , respectively). **K**, Summary of the PV interneuron SD of current ( $N=9$ ). There was no difference in the SD between baseline and AlloP (Holm–Sidak’s test,  $p=0.846$ ). 100  $\mu$ M PTX decreased the SD from baseline and AlloP (Holm–Sidak’s test,  $p=0.016$  and  $0.028$ , respectively), one-way ANOVA ( $F_{(1,403,11.22)}=10.20$ ,  $p=0.005$ ). **L**, Effects of 100 nM AlloP on the holding current in a CA1 pyramidal cell at  $-70$  mV. **M**, Summary of the tonic current in CA1 pyramidal cells. Two-way ANOVA showed no drug effect on the tonic current ( $F_{(2,24)}=1.783$ ,  $p=0.19$ ). AlloP had no effect on the tonic current in either WT or cKO CA1 pyramidal cells (Holm–Sidak’s test,  $p=0.932$  and  $0.349$ , respectively). **N**, Summary of the CA1 pyramidal neuron SD deviation of currents. Two-way

continued

ANOVA showed a drug effect on the SD ( $F_{(2,24)} = 18.04$ ,  $p < 0.0001$ ). AlloP had no effect on the SD in either WT or cKO (Holm-Sidak's test,  $p = 0.726$  and  $0.240$ , respectively).

DGCs as comparators (positive controls) with  $\delta$ -mediated tonic current that is sensitive to AlloP modulation (Fig. 5A,D). Because no synaptic stimulation was used, we expect that this protocol assays mainly the impact of tonic inhibition. We found a decrease of action potential number by AlloP in the DGCs until the maximum firing frequency was reached (Fig. 5B, top). Furthermore, AlloP decreased the membrane resistance of DGCs (Fig. 5C, top). When we applied gabazine to block GABA<sub>A</sub>Rs, AlloP did not alter the number of action potentials or the membrane resistance of PV interneurons (Fig. 5B,C, bottom). Our results indicate a direct inhibition of DGCs by AlloP through tonic inhibition. On the other hand, AlloP did not decrease the action potential number in PV interneurons (Fig. 5E). In addition, AlloP did not detectably alter the membrane resistance of PV interneurons (Fig. 5F). Taken together, 100 nM AlloP decreased the firing frequency of DGCs but had no impact on excitability of PV interneurons through tonic inhibition.

#### AlloP potentiation of phasic inhibition does not affect the firing frequency of DGCs or PV interneurons

Although AlloP has little impact on the firing frequency of PV interneurons through tonic inhibition, could the AlloP potentiation of phasic inhibition (Fig. 3) drive disinhibition of principal neurons? To test this, we injected 200-ms pulses of positive current titrated in amplitude to elicit

approximately five action potentials (Fig. 6A–D, black traces). Control sweeps were interleaved with sweeps in which we elicited phasic inhibition with extracellular stimulation (50–100  $\mu$ A) 10 ms before current injection (Fig. 6A–D, red traces). Excitation was left intact to allow feedback inhibition to participate. We titrated extracellular stimulation amplitude to reduce the number of action potentials slightly in both DGCs (Fig. 6A) and PV cells (Fig. 6C). However, in both cases, AlloP failed to increase phasic inhibition sufficiently to reliably alter firing (Fig. 6B,D, E). Furthermore, the first action potential latency showed no genotype difference between DGCs and PV interneurons. Overall, the results show that AlloP potentiation of phasic inhibition is unlikely to underlie disinhibition.

#### Limited evidence of CA1 disinhibition by neurosteroids

Several other candidate novel antidepressants, including ketamine and scopolamine, increase pyramidal cell disinhibition in hippocampus, likely by decreasing the activity of interneurons (Wohleb et al., 2016; Widman and McMahon, 2018). We reasoned that a disproportionate effect of AlloP on GABAergic inhibition of interneurons versus principal cells could have a functionally similar effect as these other novel antidepressants, although our results suggest that tonic inhibition in PVs cells is unlikely to be an important substrate for such disinhibition. To re-

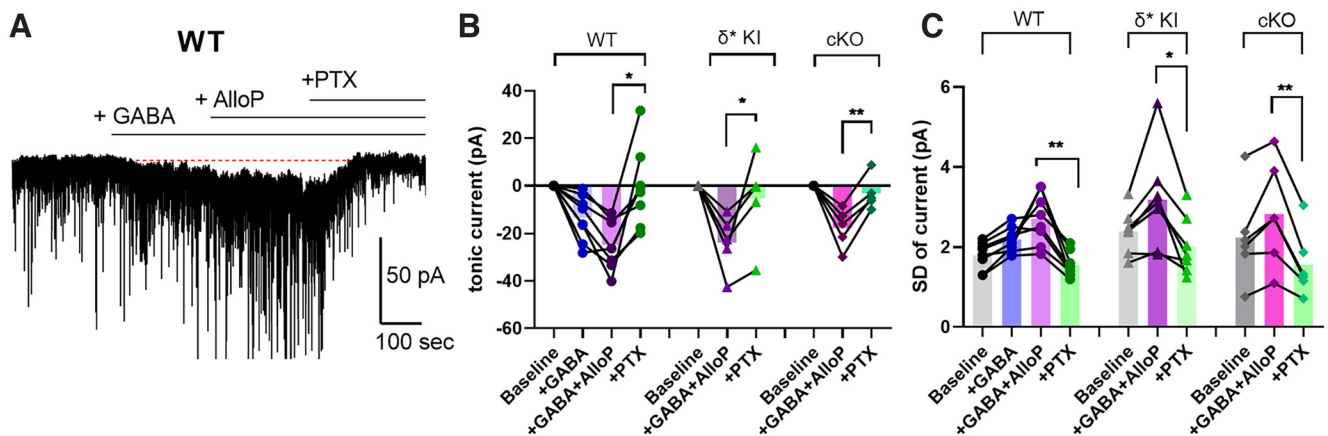


**Figure 4.** AlloP promotes tonic inhibition in the presence of 5  $\mu$ M exogenous GABA. **A**, Representative effects of 5  $\mu$ M GABA, 100 nM AlloP, and 100  $\mu$ M PTX on the holding current in a PV interneuron. **B**, Summary of changes in mean current relative to pre-GABA baseline in WT,  $\delta^*$  KI, and  $\delta$  cKO PV interneurons. In WT PV interneurons ( $N = 8$ ), one-way ANOVA showed a drug effect ( $F_{(1,942,13.6)} = 12.79$ ,  $p = 0.001$ ). GABA/AlloP potentiated a tonic current of  $-24.8$  pA, which is increased over GABA-induced current (Holm-Sidak,  $p = 0.012$ ). There is a decrease of tonic current by 100  $\mu$ M PTX (Holm-Sidak,  $p = 0.012$ ). In  $\delta^*$  KI PV interneurons ( $N = 5$ ), GABA/AlloP potentiated a tonic current of  $-23.8$  pA. 100  $\mu$ M PTX decreased GABA/AlloP potentiated tonic current (paired  $t$  test,  $p = 0.004$ ). In  $\delta$  cKO PV interneurons ( $N = 5$ ), GABA/AlloP potentiated an average of  $-17.7$  pA tonic current, which was suppressed by PTX (paired  $t$  test,  $p = 0.009$ ). **C**, Summary of the SD of current. In WT ( $N = 8$ ), one-way ANOVA showed a drug effect ( $F_{(1,330,9.311)} = 15.98$ ,  $p = 0.002$ ). There is a decrease of SD by PTX (Holm-Sidak's test,  $p = 0.016$ ). In  $\delta^*$  KI PV interneurons ( $N = 7$ ), one-way ANOVA showed a drug effect (one-way ANOVA,  $F_{(1,444,8.633)} = 11.10$ ,  $p = 0.006$ ). PTX decreased SD (Holm-Sidak's test,  $p = 0.016$ ). In  $\delta$  cKO PV interneurons ( $N = 6$ ), one-way ANOVA showed a drug effect (one-way ANOVA,  $F_{(1,642,8.212)} = 18.28$ ,  $p = 0.001$ ). PTX decreased SD (Holm-Sidak's test,  $p = 0.008$ ).



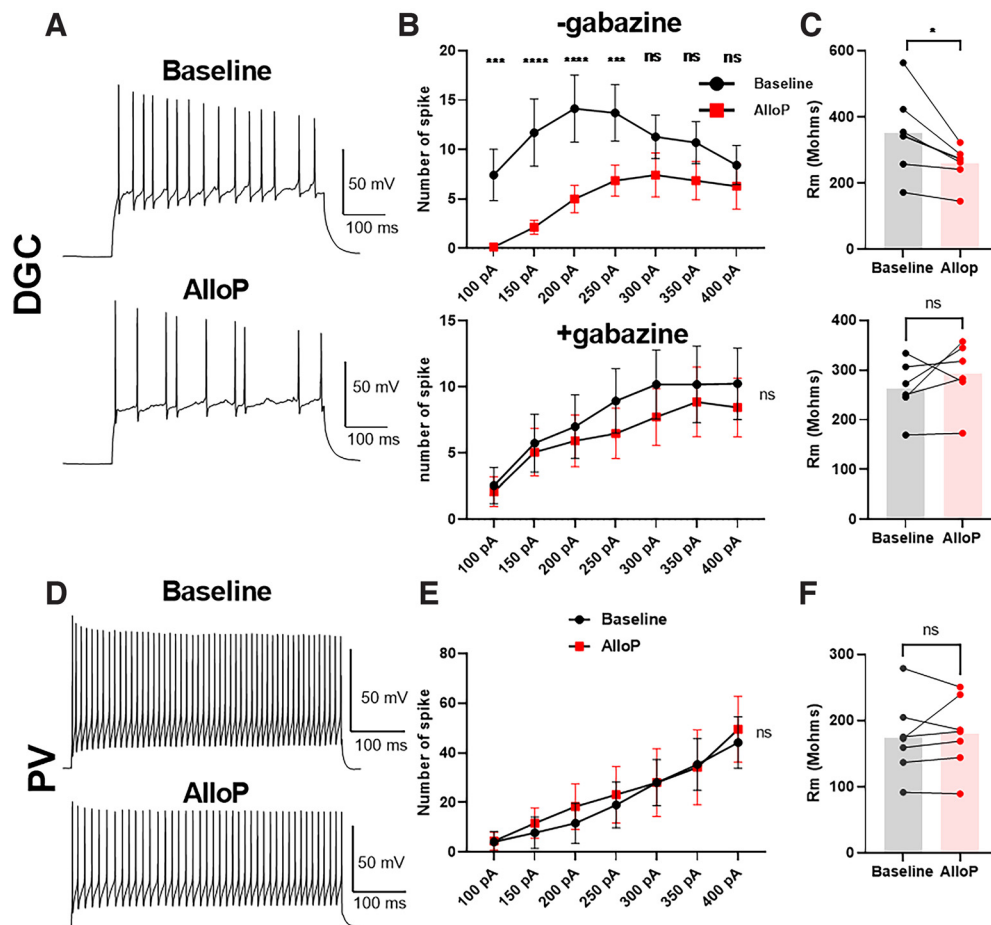


**Figure 5.** AlloP promotes inhibition of DGC firing but not PV interneuron firing. **A**, Representative action potential patterns of DGC baseline with 200 pA current injection and following application of 100 nM AlloP. **B**, Average number of action potentials in DGCs elicited at the indicated current amplitudes ( $N=8$ ). Upper panel, Two-way ANOVA on number of action potentials showed a drug effect ( $F_{(1,6)}=10.87$ ,  $p=0.017$ ). AlloP decreased the number of action potentials with 100 pA current step (Holm–Sidak,  $p < 0.001$ ), 150 pA (Holm–Sidak’s test,  $p < 0.0001$ ), 200 pA (Holm–Sidak’s test,  $p < 0.0001$ ), and 250 pA (Holm–Sidak’s test,  $p = 0.0004$ ). Lower panel, 10  $\mu\text{M}$  gabazine prevented the effect of AlloP on excitability [two-way ANOVA ( $F_{(6,30)}=1.716$ ,  $p=0.152$ )]. **C**, Upper panel, Effect of AlloP on the DGC membrane resistance. A hyperpolarization was induced by injecting  $-50$  pA current for 500 ms. Membrane resistance was calculated by dividing the final change in voltage by the current ( $N=7$ , paired  $t$  test,  $p=0.018$ ). Lower panel, In the presence of gabazine (10  $\mu\text{M}$ ), there was no consistent change in the input resistance of DGCs ( $N=6$ , paired  $t$  test,  $p=0.277$ ). **D**, Representative firing of a PV interneuron at baseline and after addition of 100 nM AlloP. **E**, Number of action potentials in PV interneurons elicited current injection ( $N=6$ ). Two-way ANOVA on number of action potentials showed no drug effect ( $F_{(1,5)}=0.227$ ,  $p=0.654$ ). **F**, No effects of AlloP on the PV interneuron membrane resistance ( $N=7$ , paired  $t$  test,  $p=0.618$ ). In **D–F**, four PV interneurons were from CA1 and three were from dentate gyrus.

investigate population excitability to synaptic stimulation, we measured the synaptic field response in the CA1 stratum pyramidale and stratum radiatum evoked via Schaffer collateral stimulation. We failed to find a reliable disinhibitory effect of 50 nM AlloP on CA1 population spikes (Fig. 7A1). Similarly, coastline burst index, a measure previously used to monitor ketamine’s effect on excitability (Widman and McMahon, 2018), failed to show an increase in excitability of CA1 pyramidal neurons with AlloP application (Fig. 7A2). On the other hand, measures of fEPSPs from dendritic field recordings revealed a small but variable increase of EPSPs by 50 nM AlloP (Fig. 7B). Similar results were obtained with 100 nM AlloP ( $1.302 \pm 0.097\%$  increase in slope,  $N=5$ ,  $p=0.035$ ).

Previous studies indicated direct inhibition from AlloP on DGCs (Stell et al., 2003; Lu et al., 2020). Consistent

with an overall inhibitory effect of AlloP in dentate gyrus, we found that fEPSPs measured in the dentate molecular layer and evoked by stimulation in the lateral perforant path, failed to show evidence of enhancement (Fig. 7C). Taken together, the results show slightly enhanced excitatory synaptic transmission with AlloP application, an effect that does not translate into increased excitability. Overall, this observation is consistent with other results herein showing little selectivity of AlloP for  $\delta$  subunit-based inhibition in interneurons.

## Discussion

In this study, we investigated the effect of the neurosteroid AlloP on tonic and phasic GABAergic inhibition in mouse hippocampal PV interneurons. Our aim was to

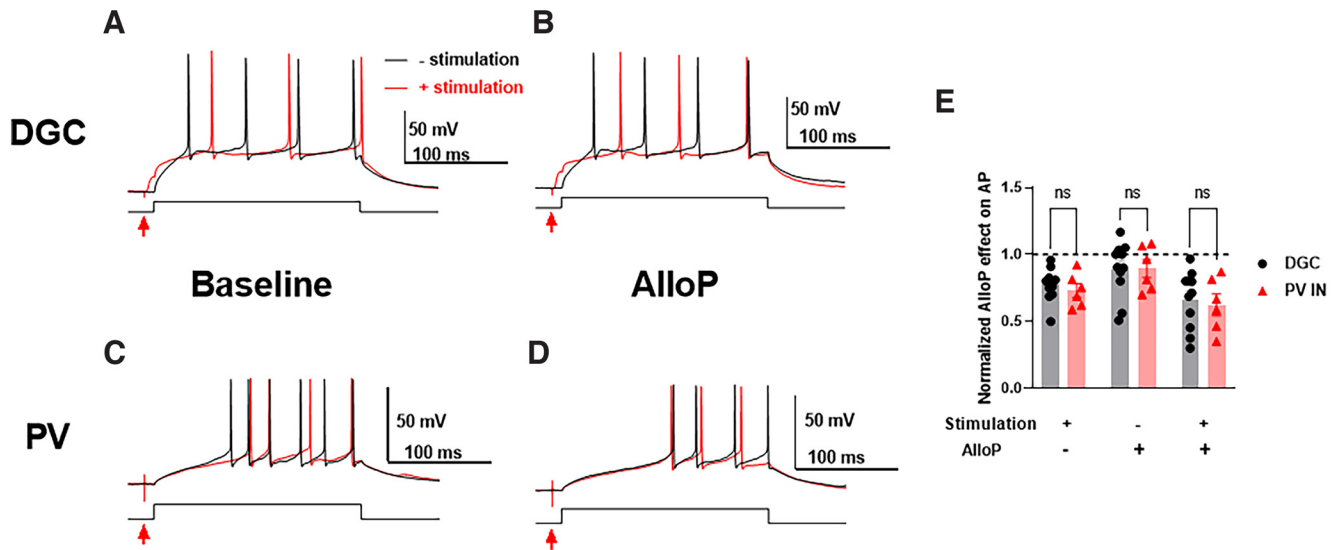


**Figure 6.** AlloP potentiation of phasic inhibition does not affect the firing frequency of DGCs or PV interneurons. **A**, Representative action potential patterns for DGC with (red traces) or without (black traces) electrical synaptic stimulation (red arrows) during baseline or **(B)** 100 nM AlloP. **C**, Representative action potential patterns of PV interneurons with or without electrical stimulation during baseline or **(D)** 100 nM AlloP. The first action potential latency showed no genotype difference between DGCs and PV interneurons [two-way ANOVA ( $F_{(1,11)} = 1.097, p = 0.3175$ )]. **E**, Normalized AlloP effect on action potentials of DGCs ( $N = 11$ ) or PV interneurons ( $N = 6$ ). Two-way ANOVA showed no genotype difference ( $F_{(1,15)} = 0.1632, p = 0.6919$ ). There is no difference for normalized action potentials between DGCs and PV INs with electrical stimulation (+), AlloP (+), or both conditions (Holm–Sidak’s,  $p = 0.955, p > 0.1$ , or  $p = 0.961$ , respectively).

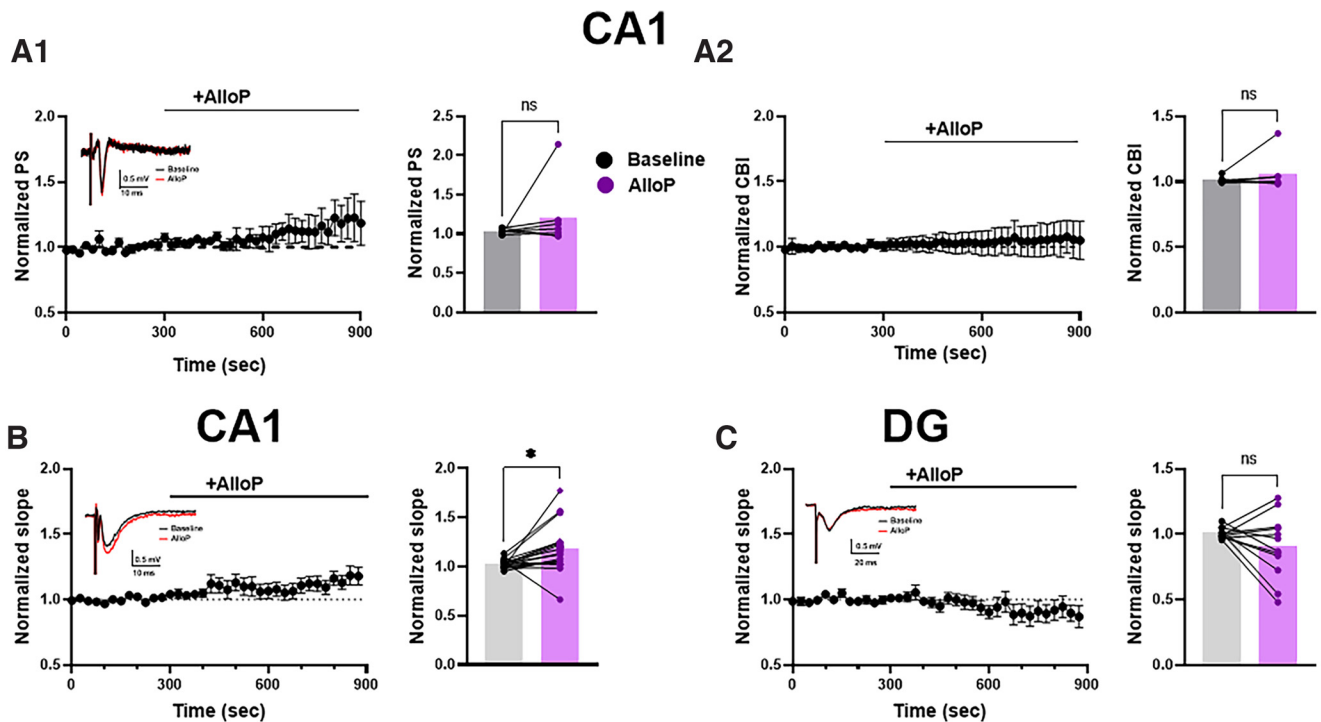


**Figure 7.** Effect of acute application AlloP on the field recordings in CA1 and DG. **A1**, Effect of 50 nM AlloP on population spike (PS) in CA1 stratum pyramidale. PS amplitude was not altered by AlloP (paired  $t$  test,  $p = 0.20, N = 7$ ). One additional recording was identified by the Prism outlier detector and excluded from analysis. **A2**, Summary of effect on fields response coastal burst index (CBI) in baseline during application of AlloP in CA1 stratum pyramidale (paired  $t$  test,  $p = 0.24, N = 8$ ). **B**, Effect of 50 nM AlloP on rising slope of fEPSP in CA1 stratum radiatum (paired  $t$  test,  $p = 0.016, N = 17$ ). No difference in the presynaptic fiber volley (paired  $t$  test,  $p = 0.234$ ). **C**, Effects of AlloP on rising slope of fEPSP in dentate gyrus (paired  $t$  test,  $p = 0.161, N = 12$ ). Sample field recordings are included as insets.

address whether AlloP at therapeutically relevant concentrations promotes activity of principal neurons through inhibition of PV interneurons. To do that, we used genetically tagged PV interneurons in mouse hippocampus and showed that AlloP promoted phasic inhibition by prolonging the decay of spontaneous IPSCs. However, AlloP promoted tonic inhibition only when co-applied with exogenous GABA, and this potentiation of tonic inhibition was not primarily through  $\delta$ -containing receptors. Furthermore, a modest AlloP concentration decreased the firing frequency of DGCs but not PV interneurons. Although AlloP modestly enhanced fEPSPs from CA1 pyramidal neurons, this effect did not translate into enhanced CA1 excitability. Thus, neither effects at the cellular nor population level indicate that hippocampal PV interneurons are a likely substrate for therapeutic AlloP effects.

### AlloP promotes phasic but not tonic inhibition on PV interneurons

The role of  $\delta$ -containing GABA<sub>A</sub> receptors in the effects of AlloP remains of interest. A previous study showed that AlloP potentiated phasic inhibition in DGCs mainly through  $\gamma$ 2-containing receptors (Lu et al., 2020), which greatly outnumber  $\delta$ -containing receptors in DGCs (Sun et al., 2018). PV interneurons also express  $\gamma$ 2-containing receptors, and these receptors should be the primary substrate of the AlloP effect on phasic inhibition in these interneurons. Surprisingly, at concentrations that prolonged phasic inhibition, AlloP did not promote tonic inhibition in PV interneurons, which we initially presumed was driven by  $\alpha$ 1/ $\delta$ -containing GABA<sub>A</sub>Rs. Previously, it was shown that  $\alpha$ 1/ $\delta$ -containing GABA<sub>A</sub>Rs have low GABA potency and efficacy (Jia et al., 2005; Jensen et al., 2013), which could explain the weak AlloP effects in PV interneurons. When AlloP was co-applied with GABA, the promotion of tonic inhibition in dentate gyrus interneurons was much lower than that in DGCs (Carver and Reddy, 2016). Indeed, AlloP potentiated tonic current in PV interneurons only when exogenous GABA was applied (Fig. 4A,B). However, when we blocked non- $\delta$  containing receptors using PTX in  $\delta^*$  KI PV interneurons, we eliminated a large amount of tonic current potentiated by GABA/AlloP (Fig. 4B,C, middle), suggesting non- $\delta$  receptor contributions. Similarly, in cKO PV interneurons, GABA/AlloP potentiated smaller but large portion of tonic current compared with those in WT (Fig. 4B,C, right). Both our KI and cKO data indicate a contribution of non- $\delta$  receptors to GABA/AlloP potentiated tonic current. However, another study showed that in basolateral amygdala, AlloP promoted tonic inhibition in PV interneurons, but not in principal cells, through  $\delta$ -containing receptors (Antonoudiou et al., 2022). This may indicate differences in subunit composition, post-translational modification of receptors, or GABA levels for PV interneurons in different brain areas important for neuropsychiatric symptoms. One mystery in our observations is the nature of baseline PTX-sensitive tonic current that is insensitive to AlloP (Fig. 3J,K). Because AlloP is a broad-spectrum modulator of GABA<sub>A</sub> subclasses, it is surprising that this current was unaffected by AlloP.

AlloP potentiates both phasic and tonic inhibition in DGCs (Lu et al., 2020). The tonic current promoted by

AlloP inhibits DGCs, increases membrane conductance, and thus reduces neuronal excitability (Fig. 5B,C). On the contrary, AlloP failed to alter excitability of PV interneurons (Fig. 5E,F), consistent with the weak effect on tonic current. It may be noteworthy that the experiment in Figure 6 failed to exhibit a tonic effect of AlloP even on DGCs, in contrast to Figure 5. We attribute this discrepancy to the briefer stimulus used to elicit action potentials in Figure 6; AlloP's tonic effects on spiking were most evident late in action potential trains in Figure 5. Regardless, neither experimental protocol revealed a detectable effect of AlloP on tonic inhibition in PV neurons.

### AlloP promotes dendritic fEPSPs in CA1

The rapid antidepressant ketamine at subanesthetic concentrations enhances population responses in hippocampal CA1 (Widman and McMahon, 2018). The promotion of dendritic fEPSPs by AlloP (Fig. 7B) indicates that AlloP could decrease tonic or feed-forward phasic inhibition from interneurons to disinhibit principal cells (Hasselmo and Schnell, 1994; Chapman et al., 1998). However, this effect did not translate into a reliable effect of AlloP on excitability measured in CA1 population spikes (Fig. 7A1,A2). Overall, the results are consistent with little to no selectivity of AlloP on inhibitory interneuron populations. The difference in fEPSP sensitivity to AlloP by hippocampal subregion might be explained by the different GABA<sub>A</sub>R subunit composition in DGCs versus CA1 pyramidal cells and by the strong overall effect of AlloP on DGCs (Lu et al., 2020) compared with interneurons (present work).

The enhanced fEPSPs in CA1 could suggest an AlloP effect on a different interneuron population, such as cholecystokinin or somatostatin interneurons, although we failed to detect a change in sIPSC frequency on CA1 pyramidal cells (Fig. 3F). Alternatively, AlloP could directly target glutamate transmission to promote modest fEPSP enhancement. Although fiber volleys were not altered, presynaptic calcium influx or AMPA receptor sensitivity could be affected.

In summary, we examined the effect of AlloP on both phasic and tonic GABAergic inhibition in PV interneurons. Our results showed that AlloP potentiated phasic inhibition through GABA<sub>A</sub>Rs. However, AlloP potentiated tonic inhibition only with exogenous GABA added, and this AlloP potentiation of tonic inhibition is not primarily through  $\delta$ -containing receptors. Furthermore, we showed AlloP had little effect on the excitability of PV interneurons. Although AlloP modestly enhanced fEPSPs from CA1 pyramidal neurons, this effect did not translate into enhanced CA1 excitability. Taken together, our work suggests that PV interneurons seem an unlikely substrate for AlloP-induced network effects through GABA<sub>A</sub> receptors, particularly those containing a  $\delta$  subunit. Other mechanisms remain to be explored to account for common antidepressant benefits of AlloP.

## References

Antonoudiou P, Colmers PLW, Walton NL, Weiss GL, Smith AC, Nguyen DP, Lewis M, Quirk MC, Barros L, Melon LC, Maguire JL (2022) Allopregnanolone mediates affective switching through

- modulation of oscillatory states in the basolateral amygdala. *Biol Psychiatry* 91:283–293.
- Brown N, Kerby J, Bonnert TP, Whiting PJ, Wafford KA (2002) Pharmacological characterization of a novel cell line expressing human  $\alpha(4)\beta(3)\delta$  GABA(A) receptors. *Br J Pharmacol* 136:965–974.
- Carver CM, Reddy DS (2016) Neurosteroid structure-activity relationships for functional activation of extrasynaptic GABA(A) receptors. *J Pharmacol Exp Ther* 357:188–204.
- Chapman CA, Perez Y, Lacaille JC (1998) Effects of GABA(A) inhibition on the expression of long-term potentiation in CA1 pyramidal cells are dependent on tetanization parameters. *Hippocampus* 8:289–298.
- Dimidschstein J, et al. (2016) A viral strategy for targeting and manipulating interneurons across vertebrate species. *Nat Neurosci* 19:1743.
- Freundl TF, Buzsáki G (1996) Interneurons of the hippocampus. *Hippocampus* 6:347–470.
- Froc DJ, Eadie B, Li AM, Wodtke K, Tse M, Christie BR (2003) Reduced synaptic plasticity in the lateral perforant path input to the dentate gyrus of aged C57BL/6 mice. *J Neurophysiol* 90:32–38.
- Glykys J, Mann EO, Mody I (2008) Which GABA(A) receptor subunits are necessary for tonic inhibition in the hippocampus? *J Neurosci* 28:1421–1426.
- Gunduz-Bruce H, Silber C, Kaul I, Rothschild AJ, Riesenberg R, Sankoh AJ, Li H, Lasser R, Zorumski CF, Rubinow DR, Paul SM, Jonas J, Doherty JJ, Kanes SJ (2019) Trial of SAGE-217 in patients with major depressive disorder. *N Engl J Med* 381:903–911.
- Harrison NL, Majewska MD, Harrington JW, Barker JL (1987) Structure-activity relationships for steroid interaction with the gamma-aminobutyric acid A receptor complex. *J Pharmacol Exp Ther* 241:346–353.
- Hasselmo M, Schnell E (1994) Laminar selectivity of the cholinergic suppression of synaptic transmission in rat hippocampal region CA1: computational modeling and brain slice physiology. *J Neurosci* 14:3898–3914.
- Herd MB, Brown AR, Lambert JJ, Belelli D (2013) Extrasynaptic GABAA receptors couple presynaptic activity to postsynaptic inhibition in the somatosensory thalamus. *J Neurosci* 33:14850.
- Hu H, Gan J, Jonas P (2014) Fast-spiking, parvalbumin<sup>+</sup> GABAergic interneurons: From cellular design to microcircuit function. *Science* 345:1252–1263.
- Jensen MLM, Wafford KA, Brown AR, Belelli D, Lambert JJ, Mirza NRN (2013) A study of subunit selectivity, mechanism and site of action of the delta selective compound 2 (DS2) at human recombinant and rodent native GABA(A) receptors. *Br J Pharmacol* 168:1118–1132.
- Jia F, Pignataro L, Schofield CM, Yue M, Harrison NL, Goldstein PA (2005) An extrasynaptic GABAA receptor mediates tonic inhibition in thalamic VB neurons. *J Neurophysiol* 94:4491–4501.
- Kanes S, Colquhoun H, Gunduz-Bruce H, Raines S, Arnold R, Schacterle A, Doherty J, Epperson CN, Deligiannidis KM, Riesenberg R, Hoffmann E, Rubinow D, Jonas J, Paul S, Meltzer-Brody S (2017) Brexanolone (SAGE-547 injection) in post-partum depression: a randomised controlled trial. *Lancet* 390:480–489.
- Ledri M, Madsen MG, Nikitidou L, Kirik D, Kokaia M (2014) Global optogenetic activation of inhibitory interneurons during epileptiform activity. *J Neurosci* 34:3364–3377.
- Lee V, Maguire J (2013) Impact of inhibitory constraint of interneurons on neuronal excitability. *J Neurophysiol* 110:2520–2535.
- Lu X, Zorumski CF, Mennerick S (2020) Lack of neurosteroid selectivity at  $\delta$  vs.  $\gamma$ 2-containing GABAA receptors in dentate granule neurons. *Front Mol Neurosci* 13:6.
- McDonald AJ, Mascagni F (2004) Parvalbumin-containing interneurons in the basolateral amygdala express high levels of the  $\alpha$ 1 subunit of the GABAA receptor. *J Comp Neurol* 473:137–146.
- Milenkovic I, Vasiljevic M, Maurer D, Höger H, Klausberger T, Sieghart W (2013) The parvalbumin-positive interneurons in the mouse dentate gyrus express GABAA receptor subunits  $\alpha$ 1,  $\beta$ 2, and  $\delta$  along their extrasynaptic cell membrane. *Neuroscience* 254:80–96.
- Pelkey KA, Chittajallu R, Craig MT, Tricoire L, Wester JC, McBain CJ (2017) Hippocampal GABAergic inhibitory interneurons. *Physiol Rev* 97:1619–1747.
- Pirker S, Schwarzer C, Wieselthaler A, Sieghart W, Sperk G (2000) GABA(A) receptors: immunocytochemical distribution of 13 subunits in the adult rat brain. *Neuroscience* 101:815–850.
- Shu HJ, Lu X, Bracamontes J, Steinbach JH, Zorumski CF, Mennerick S (2021) Pharmacological and biophysical characteristics of picrotoxin-resistant,  $\delta$  subunit-containing GABA A receptors. *Front Synaptic Neurosci* 13:763411.
- Sigel E, Steinmann ME (2012) Structure, function, and modulation of GABA(A) receptors. *J Biol Chem* 287:40224–40231.
- Smith SS, Aoki C, Shen H (2009) Puberty, steroids and GABAA receptor plasticity. *Psychoneuroendocrinology* 34:S91–S103.
- Spigelman I, Li Z, Liang J, Cagetti E, Samzadeh S, Mihalek RM, Homanics GE, Olsen RW (2003) Reduced inhibition and sensitivity to neurosteroids in hippocampus of mice lacking the GABA<sub>A</sub> receptor  $\delta$  subunit. *J Neurophysiol* 90:903–910.
- Stell BM, Brickley SG, Tang CY, Farrant M, Mody I, Mody I (2003) Neuroactive steroids reduce neuronal excitability by selectively enhancing tonic inhibition mediated by subunit-containing GABAA receptors. *Proc Natl Acad Sci U S A* 100:14439–14444.
- Struble RG, Desmond NL, Levy WB (1978) Anatomical evidence for interlamellar inhibition in the fascia dentata. *Brain Res* 152:580–585.
- Sun MY, Shu HJ, Benz A, Bracamontes J, Akk G, Zorumski CF, Steinbach JH, Mennerick SJ (2018) Chemogenetic isolation reveals synaptic contribution of  $\delta$  GABA<sub>A</sub> receptors in mouse dentate granule neurons. *J Neurosci* 38:8128–8145.
- Ting JT, Lee BR, Chong P, Soler-Llavina G, Cobbs C, Koch C, Zeng H, Lein E (2018) Preparation of acute brain slices using an optimized N-methyl-D-glucamine protective recovery method. *J Vis Exp* (132):53825.
- Walton N, Maguire J (2019) Allopregnanolone-based treatments for postpartum depression: why/how do they work? *Neurobiol Stress* 11:100198.
- Wei W, Zhang N, Peng Z, Houser CR, Mody I (2003) Perisynaptic localization of  $\delta$  subunit-containing GABAA receptors and their activation by GABA spillover in the mouse dentate gyrus. *J Neurosci* 23:10650–10661.
- Widman AJ, McMahon LL (2018) Disinhibition of CA1 pyramidal cells by low-dose ketamine and other antagonists with rapid antidepressant efficacy. *Proc Natl Acad Sci U S A* 115:E3007–E3016.
- Wohleb ES, Wu M, Gerhard DM, Taylor SR, Picciotto MR, Alreja M, Duman RS (2016) GABA interneurons mediate the rapid antidepressant-like effects of scopolamine. *J Clin Invest* 126:2482–2494.